Performance sustainability of absorption water chillier driven by solar energy in local climate of Cairo, Egypt

Mostafa Mezeyed[1], T Elnady[2], A Rashad[2] and S Elshamarqa[2]

[1] Egyptian armed forces,
[2] Military Technical Colleges, Cairo Egypt
Corresponding author E-mail: mostafamezeyed57@gmail.com

Abstract. The performance of an absorption water chillier driven by solar water heater at Egypt climate conditions was investigated. This study is implemented on a single stage absorption machine using LiBr-water working fluid to afford 8.5 ton cooling load for ABK BANK. The thermodynamic model for absorption water chillier was developed. A simulation code using Engineering Equation Solver (ESS) was developed, and was validated with data in literature. Thermodynamic analysis is assisted by the energy and mass balance of all system components. To assure the validation, the relationship between COP and both of condenser temperature and evaporator temperature was investigated. A study of case was also undertaken for the city of Cairo, Egypt. It was found that the proper working temperature of the generator for this case was 80 ^{0}C.

1. Introduction

Thermal Comfort in Domestic and Commercial activity Buildings has a significant impact on the quality of life. Based to the International Energy Agency, air conditioners and electrical fans for cooling consume approximately twenty percent of all global electrical power consumption in buildings [1]. An absorption cooling system (ACS) is a traditional cooling systems and refrigerator system that employs heating energy to generate conditioning from poor quality heating resources like energy from the sun and wasted energy [2]. Residential and conventional cooling systems rely on the vapour compression refrigeration cycle that needs power supplied by fossil fuels. The use of these fuels is harmful to the environment due to large CO2 and GHG emission levels [3-4]. The utilization of clean energy from renewable sources in cooling activities is of vital importance because it greatly minimizes the consumption of electricity and, consequently, the utilization of fossil fuels [5-7].

Water-ammonia and LiBr-water are the two most commonly used fluids to operate in ACSs. Yet, LiBr-water is widely used in air conditioners purposes [8]. Several investigators have studied single effect absorption cycle using LiBr-water as working fluids from a thermodynamic standpoint. In the absorption cooling system, the compressor is substituted by a generator, a pressure-reducing, an absorber, and a pump device. The pump consumes significantly less electricity than the compressor [9-12]. Babu and Yadav [13] evaluated the fluctuation in system COP and loads for cooling as an effect of operation temperature in ACS using a LiBr-water solution. The researchers discovered that the temperature of the evaporator must be greater than 10 °C, while the generator temperature ought to stay below 85 °C. A further investigation looked at the coefficient of performance of absorption system on a conditioning unit with an 18000 Btu/h capacity of cooling and discovered that the system's COP was 0.6 [14]. M. Yadav et al. [15] reported the simulation of absorption cooling system

using evacuated tube collectors. The researchers discovered that the COP of a system varied betwixt 0.46 and 0.78 for generator temperatures ranging from 54.4°C to 71.1°C.
J. Saucedo [16] provides a case study of creating a refrigerated system for milk storage in the city of Jalisco, Mexico, using a 5 Kw of cooling load. An ARS is activated by a geothermal heating source of 80 ◦C temperature for the single stage system and 163 ◦C for the dual stage system. The coefficient of performance of single stage system reaches to 0.85 for around $13,083, whereas the dual stage system achieved a coefficient of performance of 1.38 for $18,144. According to S. Sharifi [17], the goal of this research is to increase the coefficient of performance of a single stage of Libr-water absorption cooling system that is driven by an ETC (evacuated tube solar collector) and contrasted to a comparable system. Using the temperatures of the generator and the evaporator as variables. The data indicate an ultimate gain in energy and exergetic efficiency of around 9.1% and 3.0%, respectively. This currently amounts into a save of 187 dollars per square meters of solar collector. To achieve this upgrade, the generator's mean temperature is reduced by 6.2◦C while the evaporator's mean temperature grows by 1.6◦C.

Yu Zhou [18] utilized Aspen Plus to build an air conditioned single stage LiBr-water ARS with a capacity for cooling 23kW, adiabatic evaporation, and adiabatic absorption, and he examined the effect of temperature on the system at variable condenser temperatures. The results reveal that when the generating temperatures rise, the load rise on the solution heat exchange device progressively slows and then accelerates, whereas the load increase of other equipment decreases. After coefficient of performance of a system value becomes a certain threshold .The current research seeks to explore the performance of absorption water chillier powered by a solar water heater under all ambient conditions.

2. Theoretical Model

2.1. System Description

The absorption chillier is a single stage absorption system with an operating fluid of water-LiBr and a solar water heater fed absorption cooling system, as observed in Figure 1 with every relevant information. An ACS's main components are an absorber, a condenser, an evaporator, a generator,, a pump, a solution heat exchanger, an throttling valve and a solution throttling valve, . The concentrating mixture (including a refrigerant) is warmed by a poor-quality from source of heat in the generator, turning some of the refrigerant into vapour. The reduced solution from the generator's output is targeted toward the absorbent.
The heated vapour of refrigerant condenses in the condenser and passes into the evaporator. The decrease in pressure through the throttling valve promotes the evaporation of the refrigerant, which absorbed heat from its surroundings. The generator's weak solution passes via the solution valve for expansion and into the absorber. The vapours of refrigerant created in the evaporator flows to the absorber where it is absorbed by the weakest solution, yielding in a stronger solution. The solution pump then transports the solution to the generator, where it is warmed, and the cycle continues.

2.2. System modeling

2.2.1. Assumptions

Many implications are required to model the system [19].

- Simulations and analysis assume steady-state circumstances.
- The condenser and evaporator output refrigerants become saturated liquid and saturated vapour, respectively.
- Both generator and absorber output solutions are in balance at their separate temperature.
- All components and associated pipes exhibit zero pressure drops.
- Unless stated otherwise, heat transfer for devices and pipes are insignificant.
- The reference environment's temperature and pressure are ambient and 101kPa, respectively.

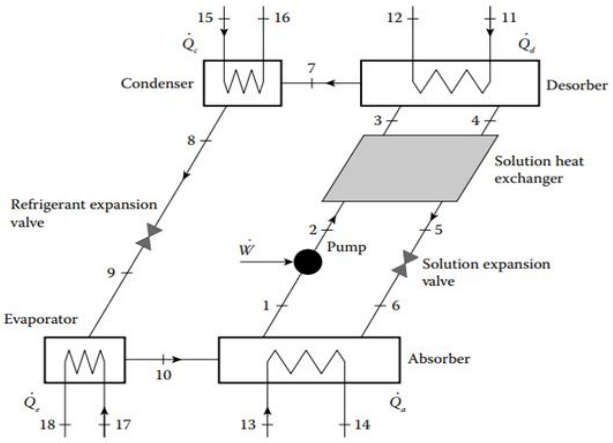

Figure 1.Graphic diagram of the modeled single stage absorption cycle

2.2.2. Thermodynamic modeling

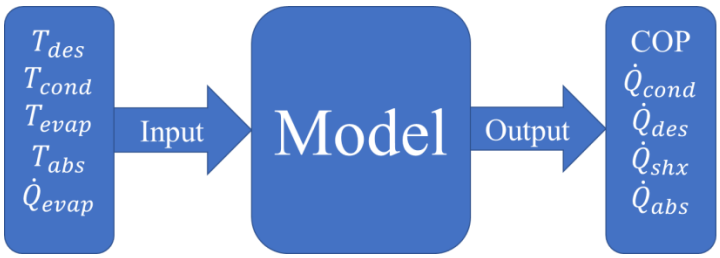

Figure 2.Graphic diagram of the modeled single stage absorption cycle

2.2.3. Energy balance

The generator's energy balance ($\dot{Q}_{gen}$):

$$\dot{Q}_{gen} = \dot{m}_4 * h_4 + \dot{m}_3 * h_3 - \dot{m}_7 * h_7 \quad (1)$$

The energy balance of the absorber device ($\dot{Q}_{abs}$):

$$\dot{Q}_{abs} = \dot{m}_{10} * h_{10} + \dot{m}_6 * h_6 - \dot{m}_1 * h_1 \quad (2)$$

The energy balance of the heat exchanger:

$$\dot{Q}_{shx} = \dot{m}_4 * h_4 - \dot{m}_5 * h_5 = \dot{m}_3 * h_3 - \dot{m}_2 * h_2 \quad (3)$$

The thermal energy is rejected into the surrounding atmosphere via the condenser ($\dot{Q}_{cond}$):

$$\dot{Q}_{cond} = \dot{m}_7 * h_7 - \dot{m}_8 * h_8 \quad (4)$$

The refrigeration product ($\dot{Q}_{evap}$):

$$\dot{Q}_{evap} = \dot{m}_{10} * h_{10} - \dot{m}_9 * h_9 \quad (5)$$

A pressure decrease in the expansion valves occurs with no heat losses; therefore its enthalpy remains constant:

$$h_6 = h_5 \quad (6)$$

$$h_9 = h_8 \quad (7)$$

Pumping work ($\dot{W}_{pump}$) can be overlooked due to its low demand:

$$h_1 = h_2 \quad (8)$$

2.2.4. Mass balance

The generator's mass flow rate balance is shown below:

$$\dot{m}_4 + \dot{m}_7 = \dot{m}_3 \quad (9)$$

$$\dot{m}_4 * X_4 = \dot{m}_3 * X_3 \quad (10)$$

Considering it assumes there is no LiBr in the evaporator outlet, a conservation of water/LiBr mixture in the absorber yields the equation below:

$$\dot{m}_1 = \dot{m}_2 = \dot{m}_3 \quad (11)$$

$$X_1 = X_2 = X_3 \quad (12)$$

$$\dot{m}_4 = \dot{m}_5 = \dot{m}_6 \quad (13)$$

$$X_4 = X_5 = X_6 \quad (14)$$

$$\dot{m}_7 = \dot{m}_8 = \dot{m}_9 = \dot{m}_{10} \quad (15)$$

$$X_7 = X_8 = X_9 = X_{10} = 0 \quad (16)$$

The heat exchanger's efficacy value is set at 80%, which is a typical number based on literature data. The performance for the absorption cycle (COP) is given as:

$$COP = \frac{\dot{Q}_{evap}}{\dot{Q}_{gen} + \dot{W}_{pump}} \quad (17)$$

Definition of the effectiveness of the solution for heat exchanger (η_{th}) follows:

$$\eta_{th} = \frac{T_4 - T_5}{T_4 + T_2} \quad (18)$$

2.2.5. Cooling tower calculation

The cooling tower is a sort of heat exchange devices that uses close proximity between air and water to chill it. The cooling tower is used to cool absorber and condenser devices.

The cooling tower's energy balance is described as:

$$\dot{Q}_{ct} = \dot{Q}_{abs} + \dot{Q}_{cond} \quad (19)$$

$$\dot{Q}_{ct} = \dot{m}_w * C_p * (T_{16} - T_{13}) \quad (20)$$

$$T_{14} = T_{15} \quad (21)$$

2.3. Validation of current work

This current work explain thermodynamic model for absorption cooling system that was validated by the confront enthalpy, pressure, temperature and capacity for all component of ACS with the published theoretical results from literature. The confront as shown in tables 1 and 2 represent percent of error between current work and the published theoretical results from literature when applying the same input parameter for the published theoretical results from literature[20].

Table 1. Comparison between current work and the published theoretical results from literature [20]

State point	Published results [20]			Current model			Enthalpy error (%)
	h (KJ/Kg)	P (Kpa)	T (℃)	h (KJ/Kg)	P (Kpa)	T (℃)	
1	85.9	0.9	35	85.29	0.8725	35	0.710128
2	85.9	7.4	35	85.29	7.385	35	0.710128
3	154	7.4	68	158.1	7.385	70.5	2.662338
4	223.3	7.4	90	224.4	7.385	90	0.492611
5	146.7	7.4	48	142.6	7.385	46	2.794819
6	146.7	0.9	48	142.6	0.8725	46	2.794819
7	2668	7.4	90	2640	7.385	90	1.049475
8	167.5	7.4	40	167.5	7.385	40	0
9	167.5	0.9	40	167.5	0.8725	40	0
10	2510	0.9	5	2510	0.8725	5	0

Table 2. Comparison between current work and the published theoretical results from literature

State point	Published results [20]	Current model	Error (%)
$\dot{Q}_{evap}$(Kw)	200	200	0
$\dot{Q}_{abs}$(Kw)	249	246.4	1.044177
$\dot{Q}_{cond}$(Kw)	212.5	211.1	0.658824
$\dot{Q}_{des}$(Kw)	261.6	257.5	1.567278
COP	0.8	0.7766	2.925

2.4. Input and design parameters for the model

This parameter is divided into two parts fixed and variable parameter. Cooling load such as a fixed parameter and evaporator, condenser, generator and absorber temperatures as a variable parameter. The parameters indicated in Table 3 represent the initial parameter for this study. Which used for getting enthalpy for each state point.

Table 3. Design conditions

Parameter	T_{evap}	T_{cond}	T_{gen}	T_{abs}	$\dot{Q}_{evap}$	η_{th}
Value	6℃	42℃	80℃	$(T_{cond} - 12)$ ℃	30 kw	0.8

2.5. Evaluation of specific enthalpies

Table 4 Shows that enthalpy terms are included, and the specific enthalpy values must be connected to the other state-point variables.

Table 4. Enthalpy of all state point

State point	Enthalpy relation	Value (kJ/kg)	Note
1	$h_1 = h(T_1, X_1)$	65.02	
2	$h_2 = h_1$	65.02	
3	$h_3 = h(T_3, X_3)$	139.3	
4	$h_4 = h(T_4, X_4)$	181.1	
5	$h_5 = h(T_5, X_5)$	100.3	
6	$h_6 = h_5$	100.3	
7	$h_7 = h(T_7, P_h)$	2632	Super-heated water vapor
8	$h_8 = h_{sat,l}(T_8)$	175.9	Saturated liquid water
9	$h_9 = h_8$	175.9	Vapor / liquid phase change
10	$h_{10} = h_{sat,v}(T_{10})$	2512	Saturated water vapor

3. Results

After simulation of the cycle, results were discussed and the relation between change of generator temperature and coefficient of performance with respect to constant evaporator temperature and variable condenser temperature was represented in fig. (3). In fig. (3), wet bulb temperature was taken as29 ^{0}C according to ASHRAE area condition, and the water was estimated to enter cooling tower at temperature 42^{0}C.

Figure (3) illustrates the relation between the coefficient of performance and generator temperature at variable condenser temperature. From figure (3), it was found that at constant condenser temperature T_{cond} the COP increases with increasing generator temperature T_{gen}. At constant generator temperature T_{gen} the COP increases with decreasing condenser T_{cond}.

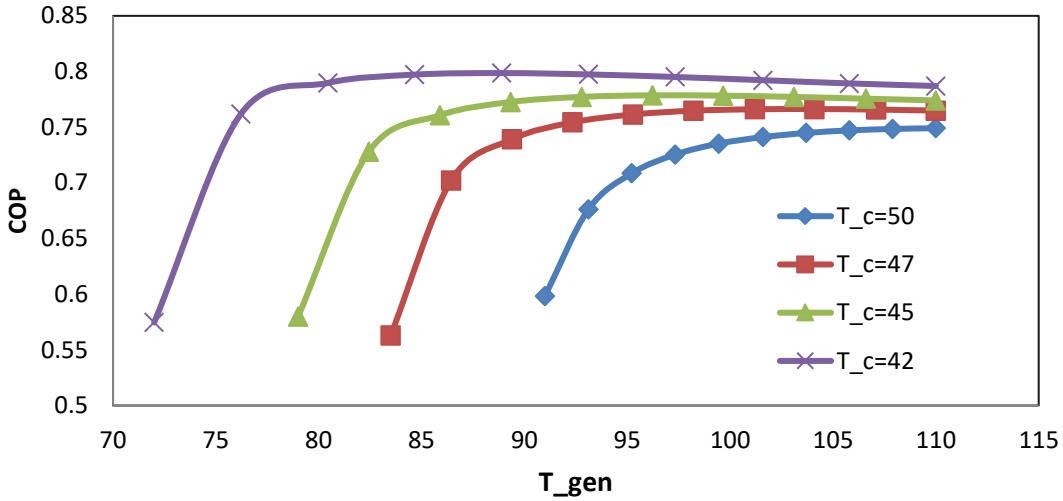

Figure 3. Relation between COP and T_{gen} at variable condenser temperature

Figure (4) illustrates the relation between the coefficient of performance and generator temperature at variable evaporator t temperature for constant condenser temperature. From figure (4), it was found that at constant evaporator temperature T_{evap} the COP increases with increasing generator temperature T_{gen}. At constant generator temperature T_{gen} the COP increases with increasing evaporator temperature T_{evap}.

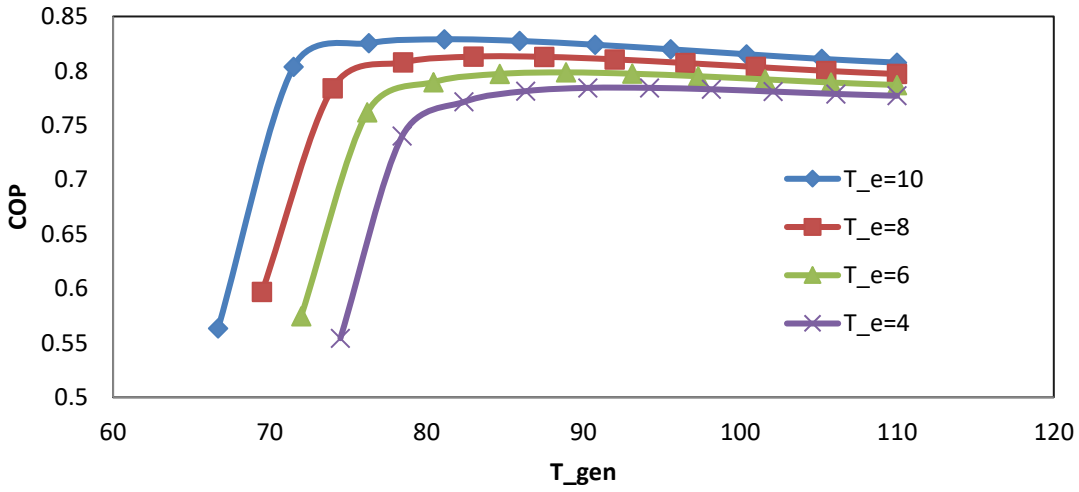

Figure 4. Relation between COP and T_{gen} at variable evaporating temperature

Choosing Cooling tower, the cooling tower characteristics were estimated as: the capacity of the cooling tower was estimated to be 92 Kw, input temperature of cooling tower is 42^{0}C and output temperature of cooling tower is 29 ^{0}C. This calculation for the initial and design parameter in table 3.

4. Conclusion

The thermodynamic design of absorption water chillier driven by solar water heater is presented and developed as a case study for the city Cairo in Egypt. This system is single stage absorption water chillier with evaporator temperature 6 ^{0}C, cooling load 30 Kw for ABK Bank, wet bulb temperature 29 ^{0}C according to ASHRAE area condition, and the water enter the cooling tower at temperature 42^{0}C. After simulation in ESS program to get the best performance of this condition, it was found that the COP increases with decreasing condenser temperatures and increasing evaporator temperatures. It was found that the proper working temperature of the generator for this case was 80 ^{o}C. This temperature is considered as a demand to operate the cycle at the design point. The next step is to design a solar field to compete with that demand. This design should be also reviewed with local climate conditions.

Nomenclature

H	Enthalpy (kJ/kg)
X	Mass fraction of LiBr
E	Emissivity
C_p	Specific heat of water (J/kg. K)
$\dot{m}$	Rate of mass flow, (kg/s)
$\dot{m}_{ct}$	Rate of mass flow of cooling tower, (kg/s)
ε_{shx}	Effectiveness of solution heat exchanger
$\dot{Q}_{cond}$	Rate of heat transfer in Condenser, (kW)
$\dot{Q}_{shx}$	Rate of heat transfer in heat exchanger, (kW)
$\dot{Q}_{ct}$	Rate of heat transfer in Cooling tower, (kW)
$\dot{Q}_{gen}$	Rate of heat transfer in Generator, (kW)
$\dot{Q}_{abs}$	Rate of heat transfer in absorber, (kW)
$\dot{Q}_{evap}$	Cooling capacity, (kW)

Abbreviation

ACS	Absorption cooling system
ETC	Evacuated tube collector
COP	Coefficient of Performance
EES	Engineering Equations Solver
SHX	Solution heat exchanger
GHG	Green House Gases

References

[1] International Energy Agency (IEA) 2018 The Future of Cooling Opportunities for energy-efficient air conditioning.

[2] Xu, D, Qu, M, Hang, Y and Zhao, F 2015 Multi-objective optimal design of a solar absorption cooling and heating system under life-cycle uncertainties *Sustain. Energy Technol. Assessments* **11** 92–105, https://doi.org/10.1016/j.seta.2015. 07.001.

[3] Elakhdar M, Tashtoush BM, Nehdi E and Kairouani L 2018 Thermodynamic analysis of a novel Ejector Enhanced Vapor Compression Refrigeration (EEVCR) cycle *Energy* **163** 1217–30 https ://doi.org/10.1016/j.energy.2018.09.050.

[4] Smith LG, Kirk GJ, Jones PJ and Williams AG 2019 The greenhouse gas impacts of converting food production in England and Wales to organic methods *Nat Commun* **10(1)** 1–10. https://doi. org/10.1038/s41467-019-12622-7

[5] Tashtoush BM, Al-Nimr MA and Khasawneh MA 2017 Investigation of the use of nano-refrigerants to enhance the performance of an ejector refrigeration system *Appl Energy* **206** 1446–63. https://doi.org/10.1016/j.apenergy.2017.09.117

[6] Chel A and Kaushik G 2018 Renewable energy technologies for sustainable development of energy efficient building *Alexandria Eng J* **57(2)** 655–69. https://doi.org/10.1016/j.aej.2017.02.027.

[7] Megdouli K, Tashtoush BM, Nahdi E, Elakhdar M, Kairouani L and Mhimid A 2016

Thermodynamic analysis of a novel ejector-cascade refrigeration cycles for freezing process applications and air-conditioning *Int J Refrig*. **70** 108–18. https: //doi.org/10.1016/j. ijrefrig.2016.06.029

[8] Misenheimer, CT and Terry, SD 2017 The development of a dynamic single effect lithium bromide absorption chiller model with enhanced generator fidelity *Energy Convers. Manage* **150** 574–587, https://doi.org/10.1016/j.enconman. 2017.08.005.

[9] Al-Shamani AN 2020 evaluation of solar-assisted absorption refrigeration cycle by using a multi-ejector *J Therm Anal Calorim*, https://doi.org/10.1007/s10973-020-09560-8.

[10] KetfO, Merzouk M, Kasbadji N and El Metenani S 2015 Performance of a single effect solar absorption cooling system *Energy Proc* **74** 130–8. https://doi.org/10.1016/j.egypro.2015.07.534

[11] Gupta A, Anand Y and Anand S 2015 Thermodynamic optimization and chemical exergy quantification for absorption-based refrigeration system *J Therm Anal Calorim* **122** 893–905. https:// doi.org/10.1007/s10973-015-4795-6

[12] Li Z, Ye X and Liu J 2014 Performance analysis of solar air cooled double effect LiBr/H2Oabsorption cooling system in subtropical city *Energy Convers Manage* **85** 302–12

[13] Babu B and Yadav GM 2015 Performance analysis of lithium-bromide water absorption refrigeration system using waste heat of boiler fuel gases *Int J Eng. Res Manag*. **2(2)** 42–7.

[14] Abdulateef J, Alghoul M, Zaharim A and Sopian K 2010 Experimental investigation on solar absorption refrigeration system in Malaysia *Renew Energy Sour* **2(3)** 267–71

[15] Yadav M and Saikhedkar NK 2017 Simulation modeling for the performance of vapor absorption refrigeration system using evacuated tube collector and parabolic disc collector working in conjugate system *Int Res J Eng. Technol*. **4(4)** 3552–8

[16] J Saucedo-Velazquez, G Guti´errez-Urueta, A Pacheco-Reyes and W Rivera 2023 Case study: Design of an absorption refrigeration system for milk preservation in Jalisco, Mexico, *Case Studies in Thermal Engineering* **44** 102866

[17] S Sharifia, F Nozad Heravi, R Shirmohammadia, R Ghasempour, F Petrakopoulou and L M Romeo 2020 Comprehensive thermodynamic and operational optimization of a solar-assisted LiBr/water absorption refrigeration system *Energy Reports* **6** 2309–2323

[18] Yu Zhou, Guihuan Yan , Xu Wang , Xiaoyang Hui, Chongqing Xu and Tao Han 2021 System simulation of air-cooling single effect LiBr absorption refrigerating system driven by solar heat source *IOP Conf. Series: Earth and Environmental Science* **766** 012005

[19] Bagheri, Shirmohammadi, Mahmoudi and Rosen 2019 Optimization and comprehensive exergy-based analyses of a parallel flow double-effect water-lithium bromide absorption refrigeration system *Appl. Therm. Eng*. **152** 643–653

[20] Bourhan Tashtoush and Husam Qaseem 2020 : An integrated absorption cooling technology with thermoelectric generator powered by solar energy. *Journal of Thermal Analysis and Calorimetry*